Modeling Line Edge Roughness in Templated, Lamellar Block Copolymer Systems

Paul N. Patrone[*,†,‡] and Gregg M. Gallatin[*,†]

Center for Nanoscale Science and Technology, National Institute of Standards and Technology, Gaithersburg, Maryland 20899, USA

E-mail: ppatrone@umd.edu; gregg.gallatin@nist.gov

Abstract

Block copolymers offer an appealing alternative to current lithographic techniques with regard to fabrication of next generation microprocessors. However, if copolymers are to be useful on an industrial manufacturing scale, they must meet or exceed lithography specifications for placement and line edge roughness (LER) of resist features. Here we use a field theoretic approach, based on the Leibler-Ohta-Kawasaki energy functional, to model the LER of lamellar microdomain interfaces in a strongly segregated block copolymer system. We consider a melt with a finite number of microdomains between parallel, template walls and derive formulas for the interface LER and sidewall angle variation (SAV) as functions of the Flory Huggins parameter χ, the index of polymerization $\mathscr{N}$, and distance from the template wall. Our perturbative approach yields explicit expressions for the dominant contributions to LER, namely, (i) an interface tension arising from the repulsive interaction between different monomer species, and (ii) a stretching energy associated with the deformation of the polymers near an interface.

[*]To whom correspondence should be addressed

[†]Center for Nanoscale Science and Technology, National Institute of Standards and Technology, Gaithersburg, Maryland 20899, USA

[‡]Department of Physics, University of Maryland, College Park, Maryland 20742-4111, USA, Institute for Research in Electronics and Applied Physics, University of Maryland, College Park, Maryland 20742, USA

Our results suggest that in order to meet the target LER goals at the 15, 11, and 6 nm nodes, χ must be increased by a factor of at least 5 above currently realized values.

1 Introduction

1.1 Background

Self-assembling block copolymers have received considerable attention in recent years, largely in the hope that they can augment state-of-the-art manufacturing techniques as microprocessor features continue to shrink.[1–4] In particular, template directed self assembly (TDSA) – the spontaneous formation of polymer microdomains between lithographically patterned boundaries – is being studied as a way to decrease the size of semiconductor features without increasing the resolution of current lithography tools (see Figure 1).[5–8] A critical task in assessing the usefulness of block-copolymers is therefore to characterize the fundamental limitations on the roughness of the patterns that they form; if the roughness cannot be controlled to within specification, devices fabricated using TDSA will have soft defects,[9] sufficient to preclude the use of block copolymers in many semiconductor manufacturing settings.

Our goal in this paper is to *analytically* predict the line edge roughness (LER) of block copolymer microdomain interfaces (cf. Figure 1) as a function of the Flory-Huggins parameter χ, the index of polymerization $\mathscr{N}$, and distance from the template; in the present analysis, we focus on lamellar systems in the strong segregation regime (SSR). Similar tasks have been pursued by, e.g. Semenov,[10] Detcheverry and de Pablo,[11–13] and Bosse,[14,15] among others;[16] however, to the best of our knowledge, these treatments either (i) relied heavily on numerical methods and computer simulations (which we do not use here), or (ii) considered geometries and physical parameters corresponding to systems in a weak segregation regime. In the context of these studies, our work is therefore motivated by two main considerations.

First, melts in the SSR are the polymer systems most relevant to a semiconductor manufacturing process. In the SSR, different types of monomers mix poorly; microdomain boundaries

are therefore sharp and well defined, which allows the microdomains to be effectively used as a template for device features (cf. Figure 1). On the other hand, polymers in the weak segregation regime exhibit significant mixing of their different monomer components, so that the geometry of microdomains becomes difficult to resolve. Second, while simulations are an invaluable tool for exploring the behavior of many complicated polymer systems, there is significant computational overhead associated with exploring the parameter space available for industrial applications. While analytic models and results do not always provide the same level of detail as simulations, they nonetheless yield insight into the physical processes affecting a system over a broad range system parameters without the computational expense associated with numerical methods. Our work therefore (i) aims to complement simulations with formulas that predict the values of χ and $\mathscr{N}$ needed to bring the LER within acceptable levels (ii) for systems that are of direct interest to the semiconductor industry.

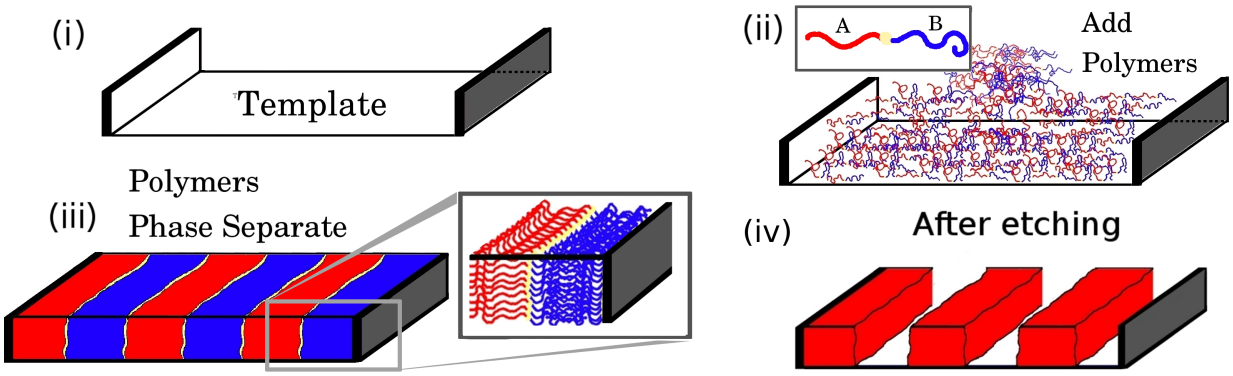

Figure 1: [Color online] A simplified cartoon showing how template directed self assembly (TDSA) can be used to pattern semiconductor devices: (i) a template is etched into a substrate using conventional lithographic techniques; (ii) block-copolymers are added to the template; (iii) polymers self organize into microdomains; (iv) by removing one of the polymer components (B components in this image) one is left with a template that can be used to guide the formation of straight wires, for example. Note that the roughness of the A-B interfaces will in principle affect the roughness of the template after etching.

The starting point of our analysis will be the phase field model originally developed by Leibler, Ohta, and Kawasaki (LOK),[17,18] which gives the energy $\mathscr{H}[\phi]$ of a polymer melt as a functional of the relative density ϕ (defined in Section 1.2) of the monomer species. In their original work,[18] Ohta and Kawasaki determined that the lowest energy configuration (for equal molecular weights

of the two monomer components) was indeed a lamellar phase-separated system, but with zero LER. Our main tasks will be to (i) determine the fluctuation eigenmodes of the system about that ground state configuration, and then (ii) construct the total LER as a weighted sum of the roughness associated with each mode; the weighting function $P[\phi]$ is given by the Bolztmann distribution,[19]

$$P[\phi] \propto e^{-\mathscr{H}[\phi]/k_B T}, \tag{1}$$

where k_B is the Boltzmann constant and T is the temperature. Interestingly, we will show that our analysis also predicts the *sidewall angle variation* (SAV).

Our choice of model is driven in large part by consideration of the features that we wish to describe. On a microscopic scale, individual polymers exhibit complicated geometries and foldings, which are adequately described by Gaussian chain models, molecular dynamics, and Monte Carlo simulations,[20–22] for example. However, for polymer melts whose domains span tens of nanometers, the computational expense of using such models becomes insurmountable, owing simply to the number of particles that must be taken into account. Moreover, at such length scales, one typically wishes to study mesoscopic features (such as the LER) of the melt as a whole, as opposed to the structure of individual molecules. Phase field models therefore enter as computationally tractable alternatives that (i) permit study of quantities relevant at the nanometer length scale, while (ii) coarse-graining microscopic features that otherwise render computation difficult. In our present analysis, we use the LOK phase field model since it is analytically tractable, and recent studies suggest that it could be well suited to describe fluctuations in technologically relevant systems.[14,15]

A salient feature of the LOK model is that it describes a system of string-like molecules (polymers composed of monomers) that *interact with each other* in terms of a macroscopic monomer density that *only interacts with a background potential*.[23] The connected nature of the polymers contributes a non-local term (which resembles an electrostatic potential) to the energy functional. As we will show, this non-local term plays an important role in limiting low frequency LER modes;

the low frequency behavior of our results will be one of the main features distinguishing them from simpler, capillary wave type models.[10,24]

We note that while the LOK model is amenable to analytic computation, it is nonetheless complicated enough that we do not find exact expressions for the LER; rather, we arrive at our final results through a series of asymptotic approximations that become increasingly accurate as the product $\chi\mathscr{N}$ increases, i.e. when the system moves further into the SSR. As a secondary benefit of this approach, the approximations we invoke will reveal the dominant physical processes that contribute to (or rather, *limit*) the LER. When possible, we will estimate the error of our approximations in terms of physical parameters describing the system.

The rest of the paper is organized as follows. In Section 2 we define the elements and key length scales of our system, review the basic principles of the LOK model, and derive the energy functional $\mathscr{H}_1$ describing fluctuations. In Section 3 we use perturbation theory to approximately diagonalize the energy functional $\mathscr{H}_1$ and identify the fluctuation modes responsible for LER and SAV. In Section 4 we define and calculate the LER and SAV. In Section 5 we discuss the physics of LER (Section 5.1), compare our results to experiments (Section 5.2) and other models (Section 5.3), and consider our main results in the context of the LER requirements set forth by the International Technology Roadmap for Semiconductors (ITRS) (Section 5.4). In Section 6, we briefly summarize our work.

1.2 Notation and Terminology

Here we summarize notation and terminology that will be used throughout the remainder of the text:

i) a is the Kuhn statistical length, which measures the average distance between two adjacent monomers. This length is considered to be extremely small relative to the system size.

ii) χ denotes the dimensionless Flory-Huggins parameter, which characterizes the repulsion between different monomer species. In passing, we note that experimentally, $\chi = \mathscr{O}(1)$ is considered to be a large value of the Flory-Huggins parameter;[25–28] this fact will become extremely

important in Section 5.4 when we discuss LER in the context of manufacturing specifications set forth by the ITRS.

iii) $\mathscr{N}$ denotes the index of polymerization, the number of monomers in a single chain.

iv) f is the (normalized) molecular weight of A monomers; $(1-f)$ is the molecular weight of B monomers.

v) $\phi(\mathrm{x}) = \phi_A(\mathrm{x}) - \phi_B(\mathrm{x})$ denotes the relative density of A monomers $[\phi_A(\mathrm{x})]$ and B monomers $[\phi_B(\mathrm{x})]$. We choose the normalization $0 \leq \phi_A(\mathrm{x}), \phi_A(\mathrm{x}) \leq 1$, so that $-1 \leq \phi \leq 1$. We furthermore impose the incompressibility condition $\phi_A(\mathrm{x}) + \phi_B(\mathrm{x}) = 1$.

vi) Ω is the physical domain of the polymer melt, whose volume will be denoted $|\Omega|$. The symbol $\mathscr{V}$ will denote a unit volume.

vii) Informally, the expression $g = \mathscr{O}(\delta)$ means that g is roughly the same size as δ.[29]

viii) Unless otherwise noted, italicized variables will represent quantities having dimensions, whereas non-italicized versions of the same variables will be dimensionless. For example, if x represents a length in some units (e.g. nm), the variable x will be a rescaled, dimensionless version of x. *The scaling of non-italicized variables will always be defined at their first appearance.*

ix) The term *pitch* (which is commonly used in lithography) will be used to refer to the average period of the polymer domain spacings; see Figure 2, for example.

2 Perspective: System Geometry, Key Parameters, and Description of Fluctuations

The system we wish to describe is a lamellar, diblock copolymer melt in the SSR (cf. Figure 2). For simplicity, we take the molecular weights of the A and B subchains to be equal (i.e. $f = 1/2$) and denote ℓ as the average width of A (or B) domains, i.e. ℓ is the so called half-pitch. We consider lamellae that have aligned themselves with parallel, template walls separated by integer multiples of the width ℓ (cf. Figure 2).[30] The parameter h denotes the height of the melt, and we assume that the system is infinite in the y direction.[31] Since the system is in the SSR, the boundaries (yellow

regions in Figure 2) between the A and B domains are small compared to ℓ.

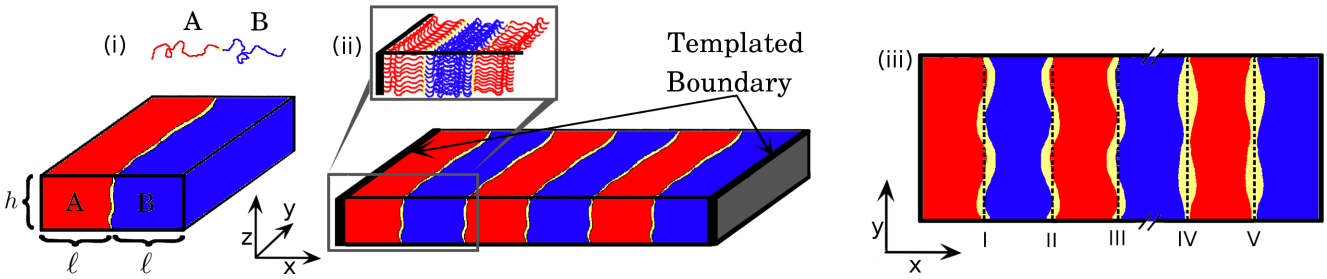

Figure 2: [Color online] Three views of a polymer melt in the lamellar phase. Inset (i) shows a single block copolymer with A (red) and B (blue) components above two microdomains comprising a full pitch; a boundary (yellow) separates regions of different monomer species. We assume that the microdomains extend to $\pm\infty$ in the y direction. Inset (ii) shows a system with three full pitches. Boundaries are located at integer values of ℓ. The closeup (gray box) illustrates how the polymers organize within the microdomains. Inset (iii) shows a top down view of a system with different types of fluctuating boundaries. The black dotted lines indicate the average positions of the microdomain boundaries. Boundaries I - III exhibit LER fluctuations corresponding to f_1 [cf. Eq. (11)]; boundaries I and II are out of phase, whereas II and III are in phase. Boundaries IV and V exhibit (in phase) SAV fluctuations, corresponding to f_2 [Eq. (12)].

We describe this system with the Leibler-Ohta-Kawasaki energy functional, an *effective* (i.e. derived) field theory that views the melt from a coarse-grained perspective. Individual polymers are not considered; rather the configuration of the system is represented by ϕ, the relative density of A and B polymers, which is a continuous function of position (see Section 1 for definition of ϕ). The energy functional takes the form,[18,23]

$$\mathscr{H}[\phi] = \frac{k_B T \chi}{\mathscr{V}} \int dV \left\{ \frac{\xi^2}{2}(\nabla\phi)^2 - \frac{\phi^2}{2} + \frac{\phi^4}{4} + \frac{\varsigma}{2} \int_\Omega dV' \phi(\mathrm{r}) g(\mathrm{r},\mathrm{r}') \phi(\mathrm{r}') \right\}, \tag{2}$$

$$\xi^2 := \frac{a^2}{3f(1-f)\chi} \qquad \varsigma := \frac{36}{f^2(1-f)^2 a^2 \chi \mathscr{N}^2}. \tag{3}$$

The function $g(\mathrm{r},\mathrm{r}')$ is the Green's function of the Laplacian. We impose periodic boundary conditions on ϕ and g in the y and z directions, which amounts to the assumption that we study the bulk behavior of the system in these two dimensions.

At the left and right x boundaries, we set $\phi = \pm 1$. More specifically ϕ has the same sign at both boundaries if the number of micrdomains is odd, but opposite signs for an even number of

microdomains; the physics is otherwise insensitive to the signs we choose, provided that the above rules are followed. Physically, these boundary conditions mean that only one monomer species will be present at any given domain wall. Experimentally this condition can be realized by making the length of the system in the x direction to be an integer value of ℓ.

We also assume that the normal derivative of g vanishes at the x boundaries, i.e. we impose Neumann boundary conditions. Physically, this choice is motivated by the observation that fluctuations at the domain boundary will have a higher energy penalty than those in the interior of the melt; at the domain wall, there are few polymers available to relieve strain caused by a fluctuation. With this in mind, we note that the Neumann condition describes the physics of the system more appropriately than a Dirichlet condition, for which $g = 0$ at the boundary.

Since we model our system using a continuum theory, we *anticipate* that the interfaces between A and B domains will be represented by *boundary layers* (cf. Figure 3), i.e. narrow regions in which the density ϕ changes rapidly. In studying interface *roughness*, therefore, our analysis will be concerned primarily with fluctuations in the position and width of these boundary layers. For perspective, we foreshadow that the parameter ξ appearing in Eq. (2) will be proportional to the the boundary layer thickness and (as we will show in the next paragraph) is small in the sense that $\xi \ll \ell$ whenever $\chi\mathcal{N} \gg 1$, when the system is in the SSR.

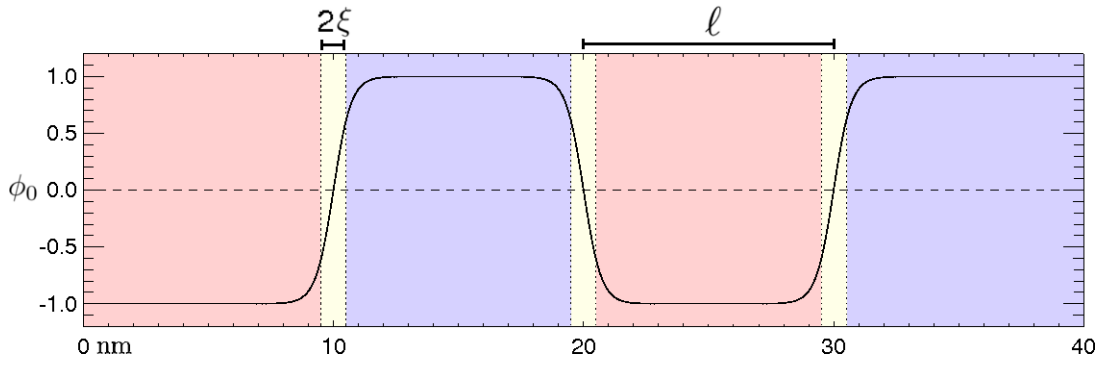

Figure 3: [Color online] The mean field density $\phi_0(x)$ [cf. Eq. (4)] for lamellar microdomains with a 10 nm half-pitch and an interface thickness $\xi = 0.5$ nm. Regions where $\phi_0 \approx +1, -1$ correspond to A-rich and B-rich microdomains, respectively. The *boundary layer* (yellow) separating A and B-rich domains has a width characterized by $\xi \ll \ell$.

The lowest energy (or mean-field) polymer density ϕ_0 may be found by taking a variational

derivative of Eq. (2) with respect to ϕ and setting the resulting first variation equal to zero. This procedure yields a complicated integro-differential equation for ϕ_0; solutions to this equation were originally pursued by Ohta and Kawasaki, who determined to a good approximation that,[18]

$$\begin{aligned} \phi_0 &= \sum_{j=1}^{N} (-1)^{j-1} \tanh\left[\frac{x - j\ell}{\sqrt{2}\xi}\right], \qquad N \text{ odd} \\ \phi_0 &= 1 - \sum_{j=1}^{N} (-1)^{j-1} \tanh\left[\frac{x - j\ell}{\sqrt{2}\xi}\right] \qquad N \text{ even} \end{aligned} \tag{4}$$

where N (not to be confused with $\mathscr{N}$, the index of polymerization) is the number of interfaces.[32] The form of ϕ_0 given above is essentially a square wave oscillating between ± 1; physically, this solution corresponds to a lamellar phase-separated system with perfectly straight interfaces having a width 2ξ (cf. Figure 3). The domain spacing ℓ was originally determined[18] by inserting Eq. (4) into Eq. (2) and minimizing the resulting expression with respect to ℓ. This procedure yields $\ell = (16\sqrt{2}/3\xi)^{1/3}(R_g)^{4/3}$ for a copolymer whose volume fraction and molecular weight are $1/2$; here $R_g = \sqrt{\mathscr{N}/2}$ is the radius of gyration.[18] The argument of the tanh functions corresponds to a choice of origin in which the mean field interface locations are at ℓ, 2ℓ, ..., as in Figure 2(ii).

If ψ is some perturbation of the mean field density, then we write $\phi = \phi_0 + \psi$ and expand Eq. (2) to second order in ψ; doing so yields,

$$\mathscr{H}[\phi] \approx \mathscr{H}[\phi_0] + \mathscr{H}_1[\psi] + \mathscr{O}(\psi^3) \tag{5}$$

$$\mathscr{H}_1[\psi] := \frac{k_B T \chi}{\mathscr{V}} \int dV \left\{ \frac{\xi^2}{2}(\nabla\psi)^2 - \frac{\psi^2}{2} + \frac{3}{2}\phi_0^2\psi^2 + \frac{\varsigma}{2}\int dV' \, \psi(\mathrm{r}) g(\mathrm{r},\mathrm{r}') \psi(\mathrm{r}') \right\}, \tag{6}$$

where $\mathscr{H}_1$ is the approximate energy of a fluctuation ψ. We require that ψ satisfy periodic boundary conditions in the y and z directions; on the x boundaries, we set $\psi = 0$. Since fluctuations with large energies should occur rarely [via Eq. (1)], the above approximation is justified for small enough temperatures by noting that the statistics of the system will be dominated by those states whose energies are near that of the ground state; in essence, we treat $|\psi|$ as a small parameter that allows for the expansion given by Eq.(6).

In general, a given state ψ of the system can be represented as a linear combination of fluctuation modes ψ_j having energy E_j (with j simply indexing the modes). In principle, however, two arbitrary fluctuation modes ψ_j and $\psi_{j'}$ will almost always be correlated, so that the amplitude of the ψ_j expressed by the system will depend on the amplitude of $\psi_{j'}$. Hence our main task is to diagonalize Eq. (6) in terms of its eigenmodes, which vary independently from one another (i.e. are uncorrelated). We can then define the LER as a linear combination of the LERs associated with each of the relevant eigenmodes.

In anticipation of this task, we examine Eq. (6) to gain insight into the types of fluctuations allowed by our model, especially since we are looking for fluctuations of *boundary layers*. The term $\xi^2(\nabla\psi)^2$ yields a (small) energy penalty for non-constant fluctuations, while the non-local term multiplying ς promotes oscillations. The pair of terms $(1/2)(3\phi_0^2-1)\psi^2$ yields an energy penalty for non-zero fluctuations *except* in the boundary layers [i.e. when $|x-n\ell| \leq \mathscr{O}(\xi)$], where these terms *promote* fluctuations. This last observation foreshadows the existence of eigenmodes localized within the microdomain interfaces, which will be responsible for LER and SAV.

3 Characterizing Interface Fluctuations

In this section, our goal is to diagonalize Eq. (6) and find the eigenmodes corresponding specifically to interface fluctuations. We begin by non-dimensionalizing space via $dV \to d\tilde{V} = dV/\xi^3$ and $\tilde{\mathrm{r}} = \mathrm{r}/\xi$. Equation (6) then becomes

$$\mathscr{H}_1[\psi] := \frac{k_B T \chi \xi^3}{\mathscr{V}} \int d\tilde{V} \left\{ \frac{1}{2}(\tilde{\nabla}\psi)^2 - \frac{\psi^2}{2} + \frac{3}{2}\phi_0^2\psi^2 + \frac{\xi^2\varsigma}{2} \int d\tilde{V}'\, \psi(\tilde{\mathrm{r}})\tilde{g}(\tilde{\mathrm{r}},\tilde{\mathrm{r}}')\psi(\tilde{\mathrm{r}}') \right\}, \tag{7}$$

where $\tilde{g}(\tilde{\mathrm{r}},\tilde{\mathrm{r}}')$ is the rescaled, dimensionless Green's function [note that $g(\mathrm{r},\mathrm{r}')$ has units of inverse length]. If ς is sufficiently small, then to leading order we may diagonalize Eq. (7) by solving the eigenvalue problem,

$$-\tilde{\nabla}^2\psi - \left[1+3\phi_0^2\right]\psi = \mathrm{E}^{(0)}\psi, \tag{8}$$

where $\mathrm{E}^{(0)}$ is a dimensionless, leading-order energy eigenvalue. We may then use standard perturbation techniques to calculate corrections to $\mathrm{E}^{(0)}$ and ψ. At the end of our analysis, we will determine the values of ς for which our perturbation theory is valid.

For a system having a single interface, Eq. (8) can be solved (up to exponentially small corrections[5]) if we cast it into the standard form,[33]

$$\psi(x,y,z) = \sum_{\mathrm{k_z}} \int \frac{d\mathrm{k_y}}{2\pi} f(\mathrm{x},\mathrm{k_y},\mathrm{k_z}) e^{i\mathrm{k_y y}+i\mathrm{k_z z}} \tag{9}$$

$$0 = \partial_{\mathrm{xx}} f + \lambda^2 f + l(l-1)\,\mathrm{sech}^2(\mathrm{x}) f, \tag{10}$$

where $\lambda^2 = 2\mathrm{E}^{(0)} - 2\mathrm{q}_\parallel^2 - 4$ and $\mathrm{q}_\parallel^2 = \mathrm{k_y}^2 + \mathrm{k_z}^2$ is a wave-vector parallel to the mean field interface profile. The constant l (not to be confused with ℓ) is an integer;[34] for the model here, $l = 3$, which is determined in the steps leading from Eq. (8) to Eq. (10). The above expressions are written in terms of the rescaled variables $\mathrm{x} = x/(\sqrt{2}\xi)$, $\mathrm{y} = y/\xi$, and $\mathrm{z} = z/\xi$. The wave-vector $\mathrm{k_y}$ is a continuous parameter (in units of ξ^{-1}), whereas $\mathrm{k_z} = 2\pi n\xi/h$, $n = 0, \pm 1, \pm 2, \ldots$ may only take discrete values.[35]

Equation (10) is in fact the well studied Pöschl-Teller equation used to model diatomic molecules in quantum mechanics; exact solutions for any l can be expressed in terms of hypergeometric functions.[36] When l takes a simple integer value, these solutions reduce to products and sums of hyperbolic and trigonometric functions. For $l = 3$, there are two "bound" state solutions (one even and one odd), which approach zero away from the interface [for $|x| > \mathscr{O}(\xi)$], and a continuous spectrum of "scattering" states that asymptote to trigonometric functions away from an interface.[37] Specifically,

$$f_1(\mathrm{x}) = \mathrm{sech}^2(\mathrm{x}), \qquad \mathrm{E}^{(0)} = \mathrm{q}_\parallel^2, \tag{11}$$

$$f_2(\mathrm{x}) = \mathrm{sech}(\mathrm{x})\tanh(\mathrm{x}), \qquad \mathrm{E}^{(0)} = \mathrm{q}_\parallel^2 + 3/2, \tag{12}$$

$$f_e(\mathrm{x}) = \frac{1}{1+\lambda^2}\left\{\left[1+\lambda^2 - 3\tanh^2(\mathrm{x})\right]\cos(\lambda\mathrm{x}) - 3\lambda\tanh(\mathrm{x})\sin(\lambda\mathrm{x})\right\}, \quad \mathrm{E}^{(0)} = \mathrm{q}_\parallel^2 + 2 + \lambda^2/2, \tag{13}$$

$$f_o(\mathrm{x}) = \frac{1}{1+\lambda^2}\left\{\left[1+\lambda^2 - 3\tanh^2(\mathrm{x})\right]\sin(\lambda\mathrm{x}) + 3\lambda\tanh(\mathrm{x})\cos(\lambda\mathrm{x})\right\}, \quad \mathrm{E}^{(0)} = \mathrm{q}_\parallel^2 + 2 + \lambda^2/2, \tag{14}$$

where f_1 and f_2 are the bound states and f_o (f_e) are the odd (even) scattering states; the associated dimensional energies $E^{(0)}$ are given by $E^{(0)} = k_B T \chi \xi^3 \mathrm{E}^{(0)}/\mathscr{V}$. The parameter λ is nonnegative, $\lambda \geq 0$. Each of these states is normalized so that the *amplitude* of the fluctuation is equal to one when $\mathrm{x} = 0$.

Since both f_1 and f_2 are localized in the boundary layer, we identify these modes as being responsible for interface fluctuations. In particular, a fluctuation of the form $\psi = f_1(\mathrm{x}) e^{i\mathrm{k_y y} + i\mathrm{k_z z}}$ corresponds to an oscillation of the interface about its mean position *without* a broadening of the width of the boundary layer; see Figure 4(iv) and Section 4. On the other hand, a fluctuation $\psi = f_2(\mathrm{x}) e^{i\mathrm{k_y y} + i\mathrm{k_z z}}$ will lead to a variation of the boundary layer (or interface) thickness; see Figure 4(v-vi). We refer to these two modes as *LER* and *SAV* fluctuations, respectively.

The solutions f_o and f_e remain non-zero over (essentially) the entire length of the system; they should be relatively high energy states, and consequently improbable. The f_o and f_e modes are fluctuations of the *composition profile*, as opposed to the interface profile.

For a system with $N > 1$ interfaces, Eq. (10) takes the approximate form,

$$0 = \partial_{\mathrm{xx}} F + \lambda^2 F + l(l-1) F \sum_{j=1}^{N} \mathrm{sech}^2[\mathrm{x} - j\mathrm{L}]\,, \tag{15}$$

where $\mathrm{L} = \ell/(\sqrt{2}\xi)$; corrections to the above expression are exponentially small. In the limit that $\xi \to 0$, we observe that Eq. (15) reduces to N copies of Eq. (8) on the domains $0 \leq x \leq 3\ell/2$, $3\ell/2 \leq x \leq 5\ell/2$, ... $(2N-3)\ell/2 \leq x \leq (2N-1)\ell/2$, $(2N-1)\ell \leq x \leq (N+1)\ell$. Asymptotically, we may then solve Eq. (15) separately on each of these domains and paste the solutions together at the boundaries. This yields the (asymptotic) bound state eigenfunctions,

$$F_i(\mathrm{x}; m) = \sum_{j=1}^{N} \Xi_j(m) f_i[\mathrm{x} - j\mathrm{L}], \tag{16}$$

where $i = 1$ or 2, and the sets $\{\Xi_j(m)\}$ are phase factors chosen to ensure that we have a complete basis of states; there are N such sets, and m is an (as of yet unspecified) quantum number. Since f_1 and f_2 are approximately zero at the points $x = 3\ell/2,\ 5\ell/2,\ ...(2N-1)\ell/2$, any orthonormal basis

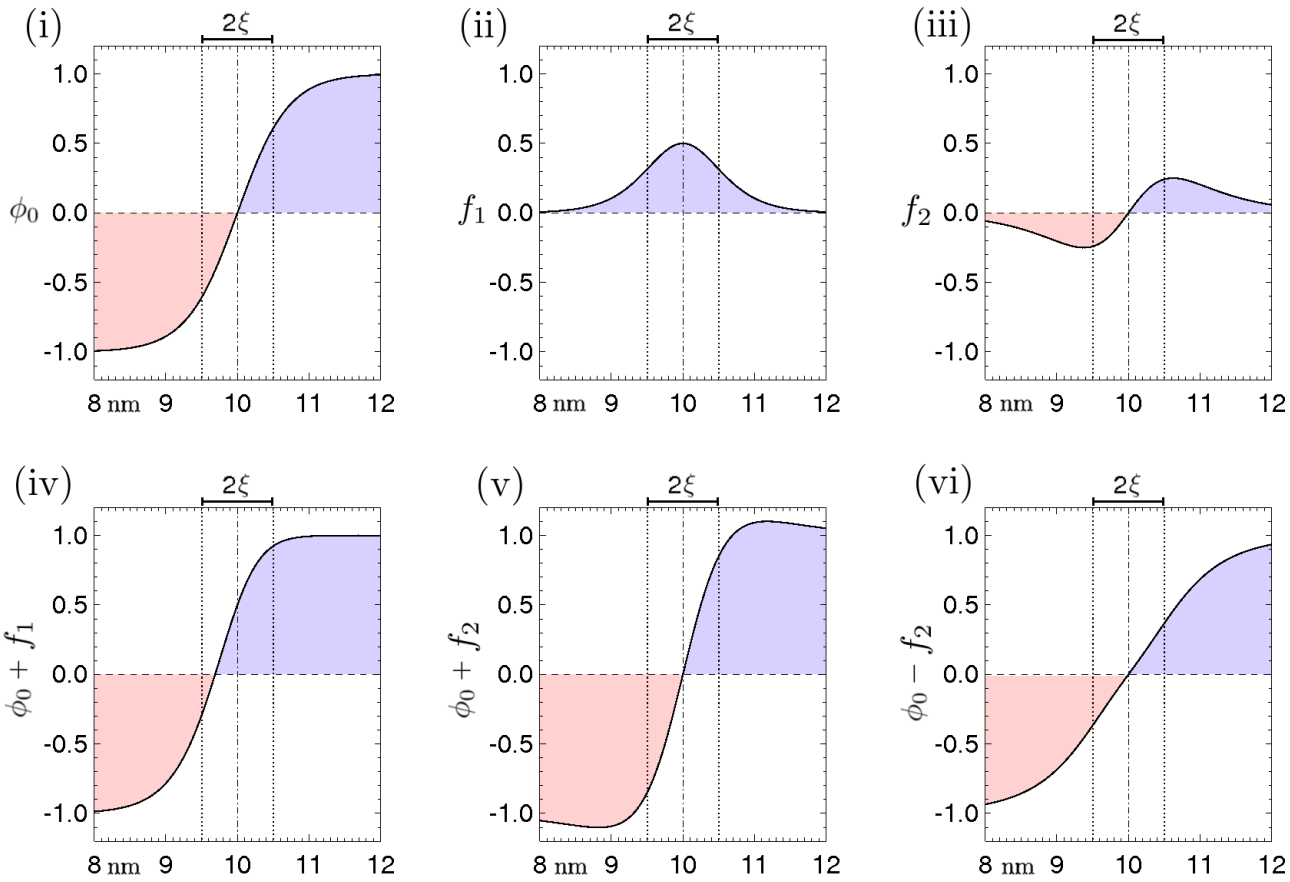

Figure 4: [Color online] The effect of fluctuation modes f_1 and f_2 on ϕ_0. In inset (i), we plot ϕ_0 for a single interface located at 10 nm with $\xi = 0.5$ nm. Insets (ii) and (iii) show the functions f_1 and f_2 localized at the interface. Inset (iv) shows that f_1 displaces the interface (i.e. the boundary layer) away from its mean position. Insets (v) and (vi) show that f_2 contracts [(v)] or expands [(vi)] the mean field interface width. As in the previous figures, red and blue shading indicates regions A and B monomer microdomains, respectively. Fluctuations of the type f_1 determine the LER, while fluctuations of the type f_2 affect the sidewall thickness or SAV.

$\{\Xi_j(m)\}$ will yield eigenfunctions $F_i(\mathrm{x};m)$ that solve Eq. (15) up to exponential corrections. An obvious choice is the Kronecker delta function basis, $\Xi_j = 1$ for $j = m$ and zero otherwise, where $1 \leq m \leq N$; that is

$$F_i(\mathrm{x};m) = f_i(\mathrm{x};m) \equiv f_i[\mathrm{x} - m\mathrm{L}]. \tag{17}$$

This basis is a set of eigenmodes corresponding to the N cases in which only one of the interfaces fluctuates.

The most natural generalization of f_o and f_e is

$$f_o(\mathrm{x};\lambda) = \frac{1}{1+\lambda^2}\left\{\left(1+\lambda^2-3\phi_0^2\right)\cos(\lambda \mathrm{x}) - 3\lambda\phi_0\sin(\lambda \mathrm{x})\right\}, \tag{18}$$

$$f_e(\mathrm{x};\lambda) = \frac{1}{1+\lambda^2}\left\{\left(1+\lambda^2-3\phi_0^2\right)\sin(\lambda \mathrm{x}) - 3\lambda\phi_0\cos(\lambda \mathrm{x})\right\}, \tag{19}$$

where we restrict λ to values for which $f_{o(e)}(0) = f_{o(e)}(N\mathrm{L}) = 0$. These solutions solve Eq. (15) up to exponentially small corrections. Since we are interested solely in fluctuations of the boundary layer, we will omit the f_o and f_e modes when writing Eq. (7) in diagonal form. Moreover, it can be shown that the amplitude of these modes will have little effect on the boundary layer since they are suppressed by a factor of ξ/ℓ relative to the f_2 fluctuations.

From perturbation theory, it is well known that the first order correction to the energy eigenvalues can be written in general as $\int dV \Psi \hat{H} \Psi$, where $\hat{H}$ is some perturbing potential, and Ψ is a (real) eigenfunction of the leading order problem.[38] In our case, we find,

$$\mathrm{E}_1^{(1)}(m, q_\parallel) \approx G(m\ell, m\ell) = \frac{\pi}{hq_\parallel}\left\{\frac{\cosh[q_\parallel \ell N] + \cosh[q_\parallel(\ell N - 2\ell m)]}{\sinh(\ell N q_\parallel)}\right\}, \tag{20}$$

$$\mathrm{E}_2^{(1)}(m, q_\parallel) \approx 0, \tag{21}$$

where $\mathrm{E}_1^{(1)}$ and $\mathrm{E}_2^{(1)}$ are the first order energy corrections for the f_1 and f_2 states. In calculating

Eqs. (20) and (21), we approximate $f_1(x;m) \approx \sqrt{2}\xi\,\delta(x-\ell m)$ and use the definition

$$\tilde{g}(\tilde{\mathrm{r}},\tilde{\mathrm{r}}') = \sum_{m=-\infty}^{\infty}\sum_{\mathrm{k_z}}\int \frac{d\mathrm{k_y}}{2\pi}\frac{e^{i\mathrm{k_z}(\mathrm{z}-\mathrm{z}')+i\mathrm{k_y}(\mathrm{y}-\mathrm{y}')}\cos(\pi m\mathrm{x}/\mathrm{L}N)\cos(\pi m\mathrm{x}'/\mathrm{L}N)}{\mathrm{k_z^2}+\mathrm{k_y^2}+(\pi m/\mathrm{L}N)^2}. \tag{22}$$

The first order energy correction for f_2 modes is approximately zero because this mode is odd and changes rapidly compared to g. It is possible to continue perturbation theory indefinitely, computing corrections to the energy eigenfunctions and eigenvalues, but for our present purposes, Eqs. (20) and (21) suffice to approximate corrections to the LER.[39]

Considering only the contributions from f_1 and f_2 fluctuations, a given state of the system is now characterized by the respective amplitudes $|C_1^{(m)}(\mathrm{q}_\parallel)|^2$ and $|C_2^{(m)}(\mathrm{q}_\parallel)|^2$ of these eigenmodes; Eq. (7) is consequently written to first order in diagonal form as,

$$\mathscr{H}_1 = \frac{k_B T h \chi \xi^2}{\sqrt{18}\mathscr{V}}\sum_n \int \frac{d\mathrm{k_y}}{2\pi}\sum_{m=1}^{N}\left\{2[\mathrm{q}_\parallel^2+G(m\ell,m\ell)]|C_1^{(m)}(\mathrm{q}_\parallel)|^2+[\mathrm{q}_\parallel^2+3/2]|C_2^{(m)}(\mathrm{q}_\parallel)|^2\right\}, \tag{23}$$

where we have (asymptotically) approximated $\int_{(m-1/2)\ell}^{(m+1/2)\ell} d\mathrm{x} f_i^2(\mathrm{x};m) \approx \int_{-\infty}^{\infty} d\mathrm{x} f_i^2(\mathrm{x};m)$. Inserting Eq. (23) into Eq. (1), gives the probability of a given fluctuation mode.

4 Defining the LER and SAV in a Continuum Setting

In Figure 3 and Figure 4 we show heuristically how the f_1 modes give rise to the line edge roughness. It is also possible to show this analytically by deriving Eq. (6) in a way that manifestly yields f_1 modes as LER fluctuations. Specifically, we assume that $\phi = \phi_0[x+\xi\zeta(y,z)]$, where $\xi\zeta(y,z)$ is a sufficiently small fluctuation of the equilibrium interface profile; expanding ϕ in powers of ξ gives

$$\phi = \phi_0[x+\xi\zeta(y,z)] \approx \phi_0(x)+\xi\phi_0'(x)\zeta(y,z)+\frac{\xi^2}{2}\phi_0''(x)\zeta(y,z)^2, \tag{24}$$

where ϕ_0', ϕ_0'' denote the first and second derivatives of ϕ_0. Substitution of Eq. (24) into Eq. (2) (with $\varsigma = 0$) then yields,

$$\mathscr{H}[\zeta] \approx \frac{k_B T \chi}{\mathscr{V}} \int dV \left\{ \frac{\xi^2}{2} \left[(f_1')^2 \zeta^2 + \frac{f_1^2}{2} (\nabla_\parallel \zeta)^2 \right] - \frac{1}{2} f_1^2 \zeta^2 + \frac{3}{2} \phi_0^2 f_1^2 \zeta^2) \right\}. \tag{25}$$

Up to a scaling of the argument of ζ, Eq. (25) is in fact just Eq. (6) with $\psi = f_1 \zeta$. Comparison to Eq. (9) reveals that Eq. (25) can be diagonalized if ζ is written as product of Fourier modes in the y and z directions. Therefore, we may conclude that f_1 modes correspond to a *shift in position* of the interface, where ξ is the physical amplitude of the actual fluctuation.[40] In passing we note that for arbitrary $\mathrm{q}_\parallel$, the direction of the interface shift will depend on z; however, when the film thickness h is small enough, the discrete k_z modes will be high energy, so that most fluctuations will be uniform throughout the height of the melt.

Based on the above analysis, we define the LER per Fourier mode $q_\parallel$ and interface m as

$$\langle \zeta_m^2(q_\parallel) \rangle = \int D[\psi] \xi^2 |C_1^{(m)}(\mathrm{q}_\parallel)|^2 P[\psi] = \frac{\mathscr{V}}{h\chi} \left[\frac{3}{2\sqrt{2}\,\xi q_\parallel^2 + 6\varsigma h G(\ell m, \ell m)} \right], \tag{26}$$

where $D[\psi]$ is a functional measure over ψ and $\mathscr{V}$ is a unit volume. We may define the LER of the mth interface in real space by integrating Eq. (26) with respect to $q_\parallel$; specifically,

$$\sigma^2(m) = \sum_n \int \frac{dk_y}{2\pi} \langle \zeta_m^2(q_\parallel) \rangle = \sum_n \int \frac{dk_y}{2\pi} \frac{\mathscr{V}}{h\chi} \left[\frac{3}{2\sqrt{2}\,\xi q_\parallel^2 + 6\varsigma h G(\ell m, \ell m)} \right]. \tag{27}$$

Note that when $\varsigma = 0$, Eq. (27) *does not* depend on m; since the f_1 modes asymptotically satisfy the homogeneous boundary conditions at $x = 0, (N+1)\ell$, the template can only affect interface fluctuations through the non-local term. Physically this makes sense; in the strong segregation regime, we expect polymer fluctuations to depend largely on the local behavior of the (mean-field) interface.

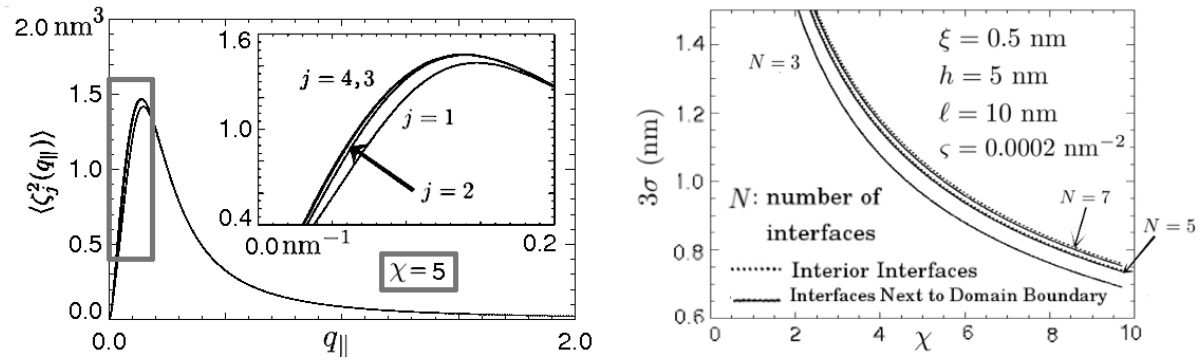

Figure 5: [Color online] LER in frequency and real space. Inset (i) shows the amplitude $\langle\zeta_j^2(q_\parallel)\rangle$ for a system with 7 interfaces, a 10 nm half-pitch, and an interface thickness $\xi = 1$ nm. Note that $\langle\zeta_j^2(q_\parallel)\rangle = \langle\zeta_{8-j}^2(q_\parallel)\rangle$. Interfaces closer to the domain boundary in general have a smaller LER than interfaces in the middle of the domain; the figure shows, however, that only the low frequency fluctuations differ significantly among interfaces. Inset (ii) shows values of 3σ given by Eq. (27); at the 11 nm node, industrial specifications require that $3\sigma \leq 1.1$ nm. Our results therefore predict that χ must be increased by at least a factor of five above previous limits in order to bring copolymers within reach of industrial specifications. This figure also shows that the *number* of microdomains has a larger impact on LER than the *position* of an interface relative to the system boundary.

In a similar manner, we may define the SAV in Fourier space as

$$\langle\tau_m^2(q_\parallel)\rangle = \int D[\psi]\xi^2|C_2^{(m)}(\mathrm{q}_\parallel)|^2 P[\psi] = \frac{\mathscr{V}}{h\chi}\frac{3\sqrt{2}\xi}{\xi^2 q_\parallel^2 + 3/2}. \tag{28}$$

Similarly, in real space,

$$\langle\tau_m^2\rangle = \sum_n \int \frac{dk_y}{2\pi}\langle\tau_m^2(q_\parallel)\rangle = \sum_n \int \frac{dk_y}{2\pi}\frac{\mathscr{V}}{h\chi}\left[\frac{3\sqrt{2}\xi}{\xi^2 q_\parallel^2 + 3/2}\right] \tag{29}$$

We note that Eqs. (27) and (29) are log divergent if we allow n and k_y to go to infinity. Following Semenov,[10] we define a cutoff frequency such that $0 \leq q_\parallel \leq 2/\xi$, which renders the integral finite and bounded; this cutoff occurs because the mean field theory breaks down for fluctuation wavelengths that are the same order of magnitude as the interface thickness.

5 Discussion

Our goals in this section are twofold. In Section 5.1, we explain the physics of LER on the basis of Eqs. (26) and (27); in the process, we discuss key approximations and limitations of our approach. In Sections 5.2 and 5.3 we compare our analysis to experimental results and other models of LER. In Section 5.4 we consider the implications of Eq. (27) in the context of manufacturing specifications set forth by the ITRS.

5.1 Physics of the LER from a Mean-Field Perspective

Equation (26) can be viewed as a consequence of the equipartition of energy law, which states that for a system in thermal equilibrium, the amplitude of a given eigenmode is *inversely proportional* to the energy of that mode. In essence, the LER is *limited* by the energy cost of deforming the interface. From that perspective, we may view the two terms in the denominator of Eq. (26) as accounting for different physical *processes* that add to this total cost.

The first of these terms, $\chi h \xi q_{\|}^2$, is an interface tension arising from the repulsive interaction between A and B monomers. This is seen by appropriately factoring the product, since, (i) ξh is the area scale associated with a x–z cross section of the interface, while (ii) for mode $q_{\|}$, the average increase in length of the interface is proportional to $q_{\|}^2$ (under a small fluctuation approximation). Therefore, a mode $q_{\|}$ will increase the number of repulsive A-B crossings (which occur in the interface region) by a factor of $h\xi q_{\|}^2$ (in a mean-field sense), with the additional factor of χ in Eq. (26) accounting for the energy cost of these crossings.

The second process described by $\chi\varsigma G(m\ell, m\ell) \sim \mathscr{N}^{-2}$ depends on the radius of gyration $R_g \sim \mathscr{N}^{1/2}$, but not χ; we conclude that this product accounts for the energy penalty of stretching or compressing the polymers in the vicinity of a fluctuating interface. This interpretation is consistent with Ohta and Kawasaki's original reason for including the non-local term $\varsigma g(\mathrm{r},\mathrm{r}')$ in Eq. (2), namely, to account for correlations arising from the connected nature of the polymers. The fact that only the diagonal elements of G appear in Eq. (26) indicates that the first order response of the

system is determined only by local re-ordering of the polymers near an interface. Continuing to higher orders in perturbation theory will in principle yield corrections proportional to $G(m\ell, m'\ell)$, i.e. energy costs associated with correlated stretching of polymers at different interfaces.

We stress that while this mean-field model provides simple physical pictures of and analytic expressions for the LER, caution should be exercised when considering systems whose half-pitch is of the order of a few nanometers. At such length scales, close examination of the parameters entering the model reveals that we push it to the limits of its validity. Notably, for a physical system in which $\xi = 1$ nm and $\ell = 10$ nm, we find that $a^2 = 3\chi\xi^2/4$, which is $\mathcal{O}(1)$ nm^2 for $\chi = 1$. Since we expect that the Kuhn length is the smallest meaningful length scale in our model, it is unclear that our analysis will be valid when $a/\xi > \mathcal{O}(1)$, or $\chi > \mathcal{O}(1)$.

The perturbation methods we use, while approximate, pose less of problem with regard to the validity of our analysis. We noted in Section 2 that the parameter ς must be small. We can estimate how small it must be from dimensional analysis; specifically, the product $\ell^2\varsigma$ should be the largest combination of terms involving ς in our perturbation analysis, so that whenever $\ell^2\varsigma \ll 1$, our analysis should be valid. We can estimate ς from its definition in Eq. (3). Taking $\xi = 1$ nm and letting $\mathcal{N} \approx 300$, we find that $\varsigma \approx (7.5 \times 10^{-3})/\chi^2$ nm^{-2}. If we use $\chi = 10$ as an upper limit suggested by our analysis, then we find $\ell^2\varsigma \approx 7.5 \times 10^{-3}$ is sufficiently small in the regimes we consider. Values as low as $\chi \approx 3$ yield $\ell^2\sigma \approx 10^{-1}$.

5.2 Comparison of our Results to Experiments

In the previous section, we showed that the LER (as predicted by the LOK mean-field model) is limited by an effective surface tension and a stretching energy. It is useful to consider the scaling behavior of these energies in a generic sense; i.e.

$$\langle \zeta^2(k) \rangle \sim (k^2 + c/k^2)^{-1}, \tag{30}$$

with c some constant and k a frequency. The second term c/k^2 is the Fourier space scaling of the Green's function (which can be understood as $g \sim \nabla^{-2}$ in real space). In the two asymptotic limits $k \to 0$ and $k \to \infty$, the LER is dominated by the stretching energy and surface tension, respectively. However, our perturbation approach implies that $c \sim \mathscr{N}^{-1/2}$, so that the contribution to the LER from the stretching energy is only apparent for very long wavelength fluctuations, for which it quickly becomes dominant. Figure 5(i) shows, for example, the asymptotic behavior of the LER power spectral density (PSD) for a 10 nm half-pitch system; the maximum occurring at $q_\parallel = \mathscr{O}(0.1)$ nm^{-1} is the approximate length scale at which the stretching energy becomes important.

Many experiments[24,41] have demonstrated a power law decay in the LER PSD with the long wavelength behavior $\langle \zeta^2(k) \rangle \sim k^{-1.6}$, as opposed to the scaling given by Eq. (30) [or Eq. (31) discussed below]. Previous works noted the disagreement between experimental and theoretical results, although to the best of our knowledge the reasons for this disagreement are still not understood.[24] Moreover, these experiments did not indicate a sharp drop as $q_\parallel \to 0$. However, in the case of Reference (26), for example, estimates of c appearing in Eq. (30) suggest that the PSD maximum should occur near $q_\parallel = \mathscr{O}(1)$ μm^{-1}, i.e. the smallest value of $q_\parallel$ that was resolved by their experiments; hence, we do not expect the $q_\parallel \to 0$ behavior of the PSD to be evident in the analysis of their data. In general, the stretching energy should become more important as the half-pitch becomes smaller, since $\varsigma \sim \mathscr{N}^{-2}$ becomes larger in this limit (c.f. also Figure 5).

5.3 Comparison of our Results to Other Models

Starting from the LOK energy functional Eq. (2), Bosse[14] studied the steady state (or equilibrium) LER of lamellar interfaces using a series of stochastic simulations based on a Cahn-Hilliard update equation for the density ϕ; however, he introduced subtleties that affect the LER PSD. Specifically, his analysis is equivalent to solving the eigenvalue equation $E\phi = \nabla^2(\delta\mathscr{H}[\phi]/\delta\phi)$, where $\delta\mathscr{H}[\phi]/\delta\phi$ indicates a variational derivative of $\mathscr{H}$ with respect to ϕ; our analysis omits the extra factor of ∇^2. The inclusion of this factor eliminates the singular behavior of PSD as $q_\parallel \to 0$;

viz. his equilibrium PSD scales like

$$\zeta(k) \sim (k^4 + c)^{-1}, \tag{31}$$

which approaches a positive constant when $k \to 0$ (again, c is a constant). The differences between Eqs. (30) and (31) can be detected by experimentally, although, as we have indicated above, the $k \to 0$ behavior of the system can likely only be studied for systems with half-pitches less than about 10 nm.

When the stretching energy is negligible, our model of LER reduces to another well known phase field model derived by Semenov, who found a nearly identical expression to Eq. (26) (with $\varsigma = 0$) by starting from a free energy significantly different from Eq. (2).[10,24] This fact suggests a deeper connection between the analysis of Refs. [9,21] and ours, which we explore here. Starting from his expression,

$$F[\phi_A, \phi_B] = \frac{a^2}{4\mathscr{V}} \int d\Omega \frac{(\nabla\phi_A)^2}{\phi_A} + \frac{(\nabla\phi_B)^2}{\phi_B} + \frac{4\mathscr{V}\chi}{a^2}\phi_A\phi_B, \tag{32}$$

and noting that $\phi_B = 1 - \phi_A$ and $\phi = \phi_A - \phi_B$, it is possible to write Eq. (32) as

$$F[\phi] = c \int d\Omega \left[\frac{1}{1-\phi^2}\right] \left\{ \xi^2 \frac{(\nabla\phi)^2}{2} + \frac{(1-\phi^2)^2}{4} \right\}, \tag{33}$$

where c is some constant.

Equation (33) is of the same form as Eq. (2) (with $\varsigma = 0$) *except* for the factor of $(1-\phi^2)^{-1}$ appearing in the integrand. This similarity ensures that both Eqs. (2) and (32) *have the same minimum*, as can be seen by taking a variational derivative of Eq. (32) with respect to ϕ. Specifically, if $\mathscr{L}_1 = (1-\phi^2)^{-1}$, $\mathscr{L}_2 = (\xi^2/2)(\nabla\phi)^2 + (1-\phi^2)^2/4$, and $\mathscr{L} = \mathscr{L}_1\mathscr{L}_2$, then

$$\left.\frac{\delta\mathscr{L}}{\delta\phi}\right|_{\phi=\phi_0} = \mathscr{L}_2 \left.\frac{\delta\mathscr{L}_1}{\delta\phi}\right|_{\phi=\phi_0} + \mathscr{L}_1 \left.\frac{\delta\mathscr{L}_2}{\delta\phi}\right|_{\phi=\phi_0} = 0, \tag{34}$$

by virtue of the fact that ϕ_0 minimizes $\mathscr{L}_2$ and $\mathscr{L}_2[\phi_0] = 0$; therefore, ϕ_0 is also a minimum of Eq. (32).

The factor of $(1-\phi^2)^{-1}$ appearing in Eq. (32) necessarily leads to a different equation for the fluctuations of the system around the configuration ϕ_0. Remarkably, however, Semenov's free energy yields an equation for ψ that has the exact form of Eq. (10), but with $l = 2$ (as opposed to $l = 3$ for the LOK model). For $l \geq 2$ it is known[36] that the Pöschl-Teller has bound states analogous to the f_1 fluctuation modes, which allowed Semenov to define the LER on the basis of these interface fluctuations. The $l = 3$ case differs notably from the $l = 2$ case in that the former also predicts the existence of f_2 fluctuations while the latter does not.

5.4 LER in a manufacturing setting

The ITRS specifies that the LER must satisfy $3\sigma < 1.1$ nm at the 11 nm node. In Figure 5 we estimate values of χ that will be required to reach these goals. Using the the values $\mathscr{N} = 300$, $\xi = 1$ nm, $\ell = 10$ nm,[6] Eq. (27) predicts that values of $\chi \approx 5$ will be required to reduce the LER to within acceptable limits. These values of χ are extremely large relative to what is seen in many experiments, where typical values range from roughly 10^{-2} for PS-PMMA [poly(styrene-b-methyl methacrylate)] to 10^{-1} for PS-PDMS [poly(styrene-b-dimethylsiloxane)].[25–28,42] Although effective values of χ as large as 1 have been reported in some systems,[26] our results suggest that at least a five-fold increase in χ is necessary to reach target goals at the 11 nm node.

Our analysis reveals a connection between the LER and the number and position of microdomains between template boundaries. Figure 5(ii) provides a representative illustration showing that for fixed χ and ℓ, decreasing the number of microdomains can reduce the LER by a factor of 20% or more. On the other hand, the position of the individual microdomains within the actual system has a much smaller effect on the LER.

While the values of χ that we report here are relatively large, we caution that the analysis herein should be taken more as a qualitative estimate of the necessary system parameters as opposed to a strict, quantitative prediction. As noted in Section 5.1, we begin to push the model to the limits of

its validity when $\chi \gg 1$ and the half-pitch approaches 10 nm or less.

We end this section by noting that the Eqs. (27) and (29) reveal an interesting, although not entirely unexpected, connection between the LER and the SAV. Specifically, the mean-field interface width ξ sets the length scale of both the LER and the SAV. Physically, this is reasonable, since both quantities refer to properties of the interface itself. However, in the context of a continuum theory, where the notion of an interface itself does not arise explicitly, it is gratifying to find that all of its associated length scales are nonetheless determined by the single parameter ξ. This internal consistency suggests that despite its possible shortcomings, the LOK phase-field model can provide significant physical insight into the behavior of block copolymer systems.

6 Conclusion

In this paper, we used the Leibler-Ohta-Kawasaki phase field model to calculate the LER and SAV of microdomain interfaces for a system of lamellar block copolymers whose order is established by straight, parallel template walls; we showed how the LER depends on the Flory-Huggins parameter, index of polymerization, and position of the interface relative to the template walls. Our analysis reveals that the main contributions to LER arise from (i) a surface tension resulting from the A-B monomer repulsion, and (ii) an energy associated with stretching the polymers in the vicinity of an interface fluctuation. Using values of the $\mathscr{N}$ (the index of polymerization) and ξ the (interface thickness) that correspond roughly to an 11 nm half-pitch, we predict that the Flory-Huggins parameter χ must be increased by at least a factor of five above current experimental values in order to reach target goals for the LER set forth in the ITRS. As our analysis is concerned primarily with fluctuations in the bulk of the film (i.e. away from the top and bottom of the system), an important extension of our work is to include the effects of polymer interactions with both the substrate and the material bounding the film from above; we speculate that one can account for such effects by the introduction of a suitable surface integral to the LOK Hamiltonian.

Acknowledgements

Support for PP was provided by the National Institute of Standards and Technology American Recovery and Reinvestment Act Measurement Science and Engineering Fellowship Program Award No. 70NANB10H026 through the University of Maryland, with ancillary support from the NSF MRSEC under Grant No. DMR 05-20471. The authors also wish to thank Dionisios Margetis and Geoffrey McFadden for useful comments and discussion during preparation of this paper.

References

(1) Park, C.; Yoon, J.; Thomas, E. L., Polymer **2003,** 44, 6725-6760.

(2) Segalman, R. A.; Mater. Sci. Eng. R **2005,** 48, 191-226.

(3) Darling, S. B., Prog. Polym. Sci. **2007,** 32, 1152-1204.

(4) *International Technology Roadmap for Semiconductors, 2011 Edition*, http://www.itrs.net/Links/2011ITRS/Home2011.htm.

(5) Sanders, D. P.; Cheng, J.; Rettner, C. T.; Hinsberg, W. D.; Kim, H.; Truong, H.; Friz, A.; Harrer, S.; Holmes, S.; Colburn, M., J. Photopolym. Sci. Technol. **2010,** 23, 11-18.

(6) Jeong, J. W.; Park, W. I.; Kim, M.; Ross, C. A.; Jung, Y. S., Nano Lett. **2011,** 11, 4095-4101.

(7) Cheng, J. Y.; Rettner, C. T.; Sanders, D. P.; Kim, H.; Hinsberg, W. D., Adv. Mater. **2008,** 20, 3155-3158.

(8) Cheng, J. Y.; Ross, C. A.; Smith, H. I.; Thomas, L., Adv. Mater. **2006,** 18, 2505-2521.

(9) As opposed to a dislocation or hard defect, a *soft* defect is a deformation of a periodic structure that preserves its topology but degrades or disrupts the final device performance.

(10) Semenov, A., N., Macromolecules **1994,** 27, 2732-2735.

(11) Detcheverry, F. A.; Pike, D. Q.; Nagpal, U.; Nealey, P. F.; and de Pablo, J. J., Soft Matter **2009,** 5, 4858-4865.

(12) Detcheverry, F. A.; Pike, D. Q.; Nealey, P. F.; Müller, M.; and de Pablo, J. J., Faraday Discuss. **2010,** 144, 111-125.

(13) Daoulas, K. C.; Müller, M.; Stoyovich, M. P.; Kang, H.; de Pablo, J. J.; Nealey, P. F., Langmuir **2008,** 24, 1284-1295.

(14) Bosse, A. W., Macromol. Theory Simul. **2010,** 19, 399406.

(15) Bosse, A. W.; Lin, E. K.; Jones, R. L.; and Karim, A., Soft Matter **2009,** 5, 4266-4271.

(16) For a preliminary analytic treatment of LER, see: Patrone, P. N.; Gallatin, G. M., Proc. SPIE **2012,** 8323, 83232Q.

(17) Leibler, L., Macromolecules **1980,** 13, 1602-1617.

(18) Ohta, T.; Kawasaki, K., Macromolecules **1986,** 19, 2621-2632.

(19) The Bolztmann distribution is sometimes referred to as the Gibbs distribution or Gibbs measure. The key idea, however, is that the statistics of our system will be given by an appropriate Canonical Ensemble.

(20) Wang, Q.; Nath, S. K.; Graham, M. D.; Nealey, P. F.; de Pablo, J. J., J. Chem. Phys. **2000,** 22, 9996-10010.

(21) Forrey, C.; Yager, K. G.; Broadaway, S. P.; ACS Nano **2011,** 4, 2895-2907.

(22) Wang, Q., J. Chem. Phys. **2007,** 126, 024903.

(23) Choksi, R.; Ren., X., J. Stat. Phys. **2003**, 113, 151-176.

(24) Stein, G. E.; Liddle, J. A.; Aquila, A. L.; Gullikson, E. M., Macromolecules **2010**, 43, 433-441.

(25) Jung, Y. S.; Ross, C. A., Nano Lett. **2007**, 7, 2046-2050.

(26) Jung, Y. S.; Chang, J. B.; Verploegen, E.; Berggren, K. K.; and Ross, C. A., Nano Lett. **2010**, 10, 1000-1005.

(27) Alberda van Ekenstein, G. O. R.; Meyboom, R.; ten Brinke, G.; Ikkala, O., Macromolecules **2000**, 33, 3752-3756.

(28) Nedoma, A. J.; Robertson, M. L.; Wanakule, N. S.; Balsara, N. P., Ind. Eng. Chem. Res. **2008,** 47, 3551-3553.

(29) More precisely, $g = \mathscr{O}(\delta)$ signifies that $|g/\delta|$ is bounded from above by a constant as $\delta \to 0$.

(30) Our present analysis will be concerned with grapho-epitaxial systems, whose ordering is induced by physical template walls. In principle one could modify our starting point to account for the effects of chemo-epitaxial patterning; we speculate that this modification could be achieved by adding a suitable surface integral to Eq. (2).

(31) By converting the appropriate integrals to sums, our analysis is trivially generalized to systems that are finite in the y direction. In Section 3 we indicate where these changes should be made.

(32) More accurately, Ohta and Kawasaki found, $\phi_0 = \sum_{j=1}^{N} \Theta[x-\ell(j-1)]\,\Theta[j\ell-x]\,(-1)^{j-1} \tanh\left[\frac{x-(j-1/2)\ell}{\sqrt{2}\xi}\right]$, where $\Theta(x)$ is the Heaviside step function; the forms we give above are equal to within exponentially small corrections (when $\xi \ll \ell$) and are notationally more convenient. By "exponentially small corrections," we mean the error in an expression is smaller than the next largest term by at least a factor of $\mathscr{O}(e^{-\ell/\xi})$. For perspective, a 10 nm half-pitch with $\xi = 1$ nm would yield corrections to Eq. (11) that are at most about $e^{-10} \approx 5 \times 10^{-5}$.

(33) Note that we have shifted the center of the domain to $x = 0$, so that $-\ell \leq x \leq \ell$.

(34) We write Eq. (10) in terms of arbitrary l to emphasize a deeper connection between our model and that of Semenov.[10] In the latter, an effective Hamiltonian significantly different from Eq. (2) leads to an equation describing interface fluctuations that has the form of Eq. (10) with $l = 2$. As we will show later, the value of l plays a significant role in determining the type and number of interface fluctuations that our model can describe. In the present section we also discuss an important connection with quantum mechanics.

(35) If the system is finite in the y direction, then Eq. (9) is appropriately modified by changing the integral over $\mathrm{k_y}$ to a sum and allowing $\mathrm{k_y}$ to only take discrete values, in the same manner as $\mathrm{k_z}$.

(36) Flügge, S. In *Practical Quantum Mechanics*, 2nd ed.; Springer-Verlag Publishers: New York, Heidelberg & Berlin, 1994; p 89.

(37) Lekner, J., Am. J. Phys **2007,** 75, 1151-1157.

(38) Sakurai, J. J. In *Modern Quantum Mechanics*, Revised ed.; Tuan, S. F., Ed.; Addison-Wesley Publishing Company: New York, 1994; p 285.

(39) In the multiple interface problem, eigenstates $f_1(\mathrm{x};m)$ are degenerate, i.e. all $f_1(\mathrm{x};m)$ have the same energy for a fixed value of $\mathrm{q}_{\|}$ (the same applies to f_2 modes). From the perspective of degenerate perturbation theory, we therefore cannot use the Kronecker basis $\Xi_j(m) = \delta_{j,m}$ when looking for energy corrections beyond first order, or eigenfunction corrections beyond leading order; rather it is necessary to rewrite the $f(\mathrm{x};m)$ in a basis that is orthogonal in the non-local term. Applying the approximations that yield Eqs. (20) and (21), this procedure is achieved by solving the eigenvalue problem $\lambda\Xi_i = \sum_j G(\ell i, \ell j)\Xi_j$ which yields an orthogonal set of $\{\Xi_j(m)\}_{j=1}^{N}$ different from the Kronecker basis we chose here.

(40) While this procedure is useful for physically interpreting the f_1 modes, we cannot assume that an expansion having the form of Eq. (24) will yield all of the possible interface fluctua-

tion modes; in fact, the assumptions underlying Eq. (24) completely neglect the possibility of the f_2 dilations. Hence, our original analysis based on Eq. (6) is necessary to account for the full behavior of the system.

(41) Stoykovich, M. P.; Daoulas, K. Ch.; Müller, M.; Kang, H.; de Pablo, J. J.; Nealey, P. F., Macromolecules **2010,** 43, 2334-2342.

(42) Black, C. T.; Ruiz, R.; Breyta, G.; Cheng, J. Y.; Colburn, M. E.; Cuarini, K. W.; Kim, H. -C.; Zhang, Y., IBM J. Res. & Dev. **2007**, 51, 605-633.

For Table of Contents Use Only

Modeling Line Edge Roughness in Templated, Lamellar Block Copolymer Systems

Paul N. Patrone and Gregg Gallatin